Mathematical and numerical modeling of inflammation

Joshua Sullivan [*] Ivan Yotov [*]

May 25, 2006

Abstract

When the body is attacked by a bacterial infection, it initiates a series of events designed to eradicate the infection while causing minimal damage to the body. Our goal is to investigate the defenses of the organ walls to the spread of infection. To do this we have chosen to model a volume of the body that includes the organ wall, the lumen outside of it and the blood and tissue within it. We have also taken into account the varied responses of the body, and our model includes many interacting agents that are part of the infection and defense processes, including the agents that attempt to prevent the infection from breaching the organ wall. The mathematical model is based on a system of nonlinear transient partial differential equations. The numerical model is based on cell-centered finite differences in space and implicit Euler in time. The model is implemented in MATLAB, and has many visualization options to better see the progression of the infection. It is hoped that this model will help in better understanding the failure of the body's defenses in such situations as Necrotizing Enterocolitis (NEC), and eventually lead to the development of a method of prevention.

1 Introduction

The body's organs walls are designed to prevent bacterial infection from penetrating into the organ. The body also has a complicated defense system to fight off infections. It is difficult to predict how the body will react in different situations. Mathematical modeling has recently become an important tool in the understanding of the inflammatory response [1, 3, 10, 9, 7, 8].

Most of the previously developed models have been based on ordinary differential equations and have only considered transient effects. In this work we develop a

[1]Department of Mathematics, University of Pittsburgh, Pittsburgh, PA 15260, U.S.A.; partially supported by the NSF grant DMS 0411694; (jts46@pitt.edu, yotov@math.pitt.edu).

three-dimensional spatial model of inflammation. We are motivated by the following considerations:

- The physical domain has spatial dimensions and consists of different compartments, e.g., lumen, epithelial, tissue, and blood. Relevant components are present at different locations, e.g., neutrophils are only present in the blood. Therefore components do not react immediately and at all times. To take into account such delay effects, diffusion and advection processes need to be modeled to determine the spatial distribution of the reactive components.

- Some of the chemical species involved in the system move in the direction of increasing chemoattractant gradients. For example, the displacement of activated neutrophils is related to the spatial gradient of cytokines.

- Different regions of the physical domain have different material properties that affect the component transport, e.g., diffusion in blood occurs faster than diffusion in tissue.

- Epithelial cells exhibit migration, proliferation and apoptosis [6]. Cells interact through electric signals and are connected via tight junctions and gap junctions. The spatial distribution and strength of these junctions affect the permeability of the epithelial layer and the transport of bacteria through it [4].

In our studies we seek to understand the situations where the body succeeds compared to the situations in which it fails. We expect that stronger infections and/or initial organ damage will lead to sepsis where otherwise the body might fend off the infection.

Our model includes the following components that play a critical role in the inflammation process.

- e_c: epithelial cells - barrier to infection

- b: bacteria - infecting agent

- m: macrophage - stationary dormant defense system

- m_a: activated macrophage - slow attack cell of the immune system

- c: pro-inflammatory cytokine - messenger to promote response

- c_a: anti-inflammatory cytokine - messenger to hinder response

- NO: nitric oxide - waste chemical that damages the wall integrity

- $ZO1$: tight junction protein - restricts passage through the wall

- N: neutrophil - dormant defense system in the blood

- N_a: activated neutrophil - fast attack cell of the immune system
- d: damage - measure of the level of the problem

The following reactions describe the inflammation cascade.

$$m + b \xrightarrow{k_{bm}} m_a + b \quad \text{macrophage activation} \tag{1}$$
$$m_a + b \xrightarrow{k_{ab}} m_a + c \quad \text{macrophage bacteria destruction} \tag{2}$$
$$m_a \xrightarrow{k_{ma\,c}} m_a + c \quad \text{macrophage cytokine release} \tag{3}$$
$$c + m \xrightarrow{k_{cm}} m_a + NO \quad \text{macrophage reaction promotion} \tag{4}$$
$$c + N \xrightarrow{k_{cN}} N_a + N \quad \text{neutrophil reaction promotion} \tag{5}$$
$$N_a + b \xrightarrow{k_{Na}b} N_a + c \quad \text{neutrophil bacteria destruction} \tag{6}$$
$$N_a \xrightarrow{k_{Na}c} N_a + c \quad \text{neutrophil cytokine release} \tag{7}$$
$$e_c \xrightarrow{k_p} 2e_c \quad \text{proliferation of epi cells} \tag{8}$$
$$e_c \xrightarrow{k_a} * \quad \text{apoptosis of epi cells} \tag{9}$$
$$NO + ZO1 \xrightarrow{k_{nz}} NO \quad \text{tight junction destruction} \tag{10}$$
$$d + m \xrightarrow{k_{dm}} m_a \quad \text{macrophage activation from damage} \tag{11}$$
$$d + N \xrightarrow{k_{dN}} N_a \quad \text{neutrophil activation from damage} \tag{12}$$

Reactions (1), (2), (4), (5), (6), (11), and (12) are slowed down by the anti-inflammatory cytokine c_a by multiplying the reaction rates by a retardation factor $R(c_a)$ defined in (25) below.

We refer the reader to [5] for more details on the inflammatory response.

2 Mathematical model

We use partial differential equations to model the species' interactions and reactions as specified previously. In this approach the concentrations of the components are modeled as continuous functions. Spatial physical processes such as diffusion and chemotaxis are modeled by differential operators acting on the concentration functions. The equations represent conservation of mass for the various components. An alternative approach is agent-based modeling (ABM) [1] where the physical processes are modeled by a set of discrete rules.

Our model consists of the following set of time dependent partial differential equations.

$$\frac{\partial e_c}{\partial t} + \nabla \cdot (\beta(e_c)\mathbf{u}(e_c, b)) = k_p e_c(1 - e_c/e_c^{max}) - k_a(b)e_c \tag{13}$$

$$\beta(e_c) = \frac{e_c^2}{e_c^2 + (e_c^{max} - e_c)^2}, \quad \mathbf{u}(e_c, b) = -\alpha(b)\nabla e_c \tag{14}$$

$$\frac{\partial b}{\partial t} - \nabla \cdot D_b \nabla b = k_{bg} b(1 - b/b_{max}) - k_b b/(1 + b/\epsilon) - R(c_a)(k_{ab} m_a b + k_{N_a b} N_a b) \tag{15}$$

$$\frac{\partial m}{\partial t} = k_{m0} m_0 (1 - m/m_{max}) - k_m m - R(c_a)(k_{bm} bm + k_{cm} cm + k_{dm} dm) \tag{16}$$

$$\frac{\partial m_a}{\partial t} - \nabla \cdot (D_{m_a} \nabla m_a - \gamma_0 m_a \nabla c - \gamma_1 m_a \nabla b) = -k_m m_a + R(c_a)(k_{bm} bm + k_{cm} cm + k_{dm} dm) \tag{17}$$

$$\frac{\partial c}{\partial t} - \nabla \cdot D_c \nabla c = -k_c c + k_{m_a c} m_a + k_{N_a c} N_a + R(c_a)(k_{ab} m_a b + k_{N_a b} N_a b - k_{cN} cN - k_{cm} cm) \tag{18}$$

$$\frac{\partial c_a}{\partial t} - \nabla \cdot D_{c_a} \nabla c_a = -k_{c_a} c_a + s_c + k_{cnn} \frac{Q}{1 + Q} \tag{19}$$

$$\frac{\partial NO}{\partial t} = -k_{no} NO + k_{cm} cm \tag{20}$$

$$\frac{\partial ZO1}{\partial t} = k_{zo1}\, h(e_c, e_c^{max}, 1/4) ZO1_0 (1 - ZO1/ZO1_{max}) - k_{nz} NO * ZO1 \tag{21}$$

$$\frac{\partial N_a}{\partial t} - \nabla \cdot (D_{N_a} \nabla N_a - \gamma_2 N_a \nabla c) = -k_{N_a} N_a + R(c_a)(k_{cN} cN + k_{dN} dN) \tag{22}$$

$$\frac{\partial d}{\partial t} - \nabla \cdot D_d \nabla d = -k_d d + k_{dn} \frac{T^q}{x_{dn}^q + T^q} \tag{23}$$

$$\gamma_1 >> \gamma_0, \quad T = \frac{m_a + N_a}{1 + k_{nc}(c_a/\bar{c}_a)^2}, \quad Q = \frac{m_a + N_a + k_{cnd} d}{1 + k_{nc}(c/\bar{c}_a)^2} \tag{24}$$

$$R(c_a) = \frac{1}{1 + k_{nc}(c_a/\bar{c}_a)^2}, \quad h(a, b, q) = \frac{a^q}{a^q + (b - a)^q} \tag{25}$$

Some of the reactions in the above model have been developed in [7, 8].

Physical domain: The domain Ω is 3-dimensional and consists of four horizontal regions. The regions from top to bottom are lumen Ω_1, epithelial layer Ω_2, tissue region Ω_3 and circulatory system Ω_4.

Initial Conditions:

$$e_c = e_c^{max} \text{ in } \Omega_2,\ e_c = 0 \text{ in } \Omega_1 \cup \Omega_3 \cup \Omega_4,$$

$$b = b_0 \text{ in } \Omega_1, b = 0 \text{ in } \Omega_2 \cup \Omega_3 \cup \Omega_4,$$

$$m = 0 \text{ in } \Omega_1, m = m_{max} \text{ in } \Omega_2 \cup \Omega_3 \cup \Omega_4,$$

$$m_a = 0,\ c = 0,\ NO = 0,\ N_a = 0 \text{ in } \Omega,$$
$$ZO1 = ZO1_{max} \text{ in } \Omega_2,\ ZO1 = 0 \text{ in } \Omega_1 \cup \Omega_3 \cup \Omega_4,$$
$$N = 0 \text{ in } \Omega_1 \cup \Omega_2 \cup \Omega_3,\ N = N_0 \text{ in } \Omega_4.$$

Boundary Conditions. Zero diffusive flux, $D_b \nabla b \cdot n = 0$, where n is the outward unit normal vector, is imposed on the top and bottom faces. Periodic boundary conditions are used on the rest of the boundary.

Modeling of the epithelial layer permeability. The epithelial layer permeability depends on the amount of the tight junction protein $ZO1$. This is modeled by multiplying the vertical diffusion coefficients on the interface between the epithelial layer and the tissue by a permeability function, e.g.,

$$D_b^z \leftarrow D_b^z\, h(ZO1_{max} - ZO1, ZO1_{max}, 2).$$

Similarly the blood/tissue barrier is generally very restrictive unless it is damaged:

$$D_b^z \leftarrow D_b^z\, h(d - d_{max}, d_{max}, 2).$$

The same modifications are done for $D_{m_a}^z$, D_c^z, and $D_{N_a}^z$.

Epithelial cell modeling.

- The e_c equation is a conservation law with nonlinear flux $\beta(e_c)\mathbf{u}(e_c, b)$. Note that
$$\nabla \cdot (\beta(e_c)\mathbf{u}(e_c, b)) = \nabla\beta(e_c) \cdot \mathbf{u} + \beta(e_c)\nabla \cdot \mathbf{u}(e_c, b),$$
$$\nabla\beta(e_c) \cdot \mathbf{u} = \beta'(e_c)\mathbf{u} \cdot \nabla e_c \qquad \text{advection},$$
$$\beta(e_c)\nabla \cdot \mathbf{u}(e_c, b) = -\beta(e_c)\nabla \cdot (\alpha(b)\nabla e_c) \qquad \text{diffusion}$$
The choice of $\beta(e_c)$ comes from the Buckley-Leverett model of two-phase flow [2]. It is S-shaped and leads to no advection for $e_c = 0$ and $e_c = e_c^{max}$. Note that the advection depends on $\beta'(e_c)$. The vector $\mathbf{u}$ is a velocity vector, which is proportional to $-\nabla e_c$, therefore $\nabla \cdot \mathbf{u}$ models diffusion.

- Cell migration is affected by the presence of LPS. LPS is endotoxin present in the lumen bacteria. Its presence leads to increased function of integrins in the cells, causing them to stick too strongly to the matrix and thus impairing migration, see [6]. This is modeled by taking
$$\alpha(b) = \gamma_3\, h(b, b_{max}, 1/2).$$
When $b = b_{max}$, no migration of cells occurs.

- The apoptosis rate $k_a(b)$ is an increasing function of b, e.g., $k_a(b) = h(b, b_{max}, 0.25)$.

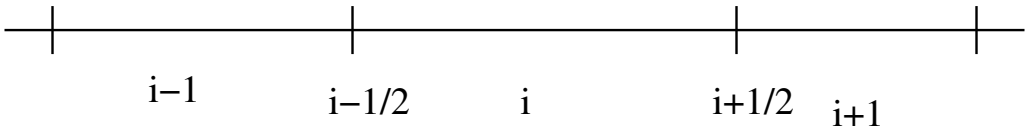

Figure 1: Grid

3 Numerical model

The domain is discretized by a rectangular but not necessarily uniform grid. We use backward Euler in time and cell-centered finite differences in space. Each cell is associated with one of the materials of the domain. The diffusion coefficients are given at the cell centers. The discretization requires their values at the midpoints of the faces. These are computed by harmonically averaging the values at the neighboring cells.

The nonlinear algebraic system arising from the implicit scheme on each time step is solved by a fixed-point root-finding iteration. By changing the number of iterations, we can vary the level of implicitness - one iteration corresponds to explicit (forward) Euler.

Discretization of the epithelial cells equation. Consider $\frac{\partial}{\partial x}$; the other derivatives are treated similarly. Denote the grid cells by i with midpoints m_i and the grid vertices by $x_{i-1/2}$, see Figure 1. Let $h_i = x_{i+1/2} - x_{i-1/2}$ and $h_{i-1/2} = m_i - m_{i-1}$. On cell i:

$$\frac{\partial}{\partial x}(\beta(e_c)u_x(e_c,b)) = \frac{1}{h_i}(\beta^{i+1/2}(e_c)u_x^{i+1/2}(e_c,b) - \beta^{i-1/2}(e_c)u_x^{i-1/2}(e_c,b)),$$

where

$$u_x^{i+1/2}(e_c,b) = -\frac{1}{2}(\alpha(b_i)+\alpha(b_{i+1}))\frac{e_{c,i+1}-e_{c,i}}{h_{i+1/2}},$$

$$u_x^{i-1/2}(e_c,b) = -\frac{1}{2}(\alpha(b_{i-1})+\alpha(b_i))\frac{e_{c,i}-e_{c,i-1}}{h_{i-1/2}}.$$

Use upwinding for $\beta(e_c)$:

$$\beta^{i+1/2}(e_c) = \begin{cases} \beta(e_{c,i}) & \text{if } u_x^{i+1/2} \geq 0, \\ \beta(e_{c,i+1}) & \text{if } u_x^{i+1/2} < 0 \end{cases}$$

$$\beta^{i-1/2}(e_c) = \begin{cases} \beta(e_{c,i-1}) & \text{if } u_x^{i-1/2} \geq 0, \\ \beta(e_{c,i}) & \text{if } u_x^{i-1/2} < 0 \end{cases}$$

4 Simulation results

The model handles differing sets of initial conditions, rates, etc. We study two special cases.

- Case 1: differing amounts of bacteria can affect the ability of a damaged epithelial wall to heal itself.
- Case 2: differing strains of bacteria can either lead to sepsis or be wiped out by the immune system based on the strength of the bacterial strain.

We use the following parameter values obtained in [8]:

$$k_d = .02,\ k_{dn} = 0.35,\ x_{dn} = .06,\ q = 6,\ k_{cnd} = 48,\ \bar{c}_a = 0.28,\ k_c = 0.1,\ k_{nc} = 1,$$

$$k_{cnn} = .04,\ s_c = 0.0125,\ k_{N_a} = 0.05, k_{N_ab} = 1.8,\ k_{bg} = 0.3,\ k_b = 1.5,\ \epsilon = 0.2.$$

Note that the bacteria growth rate k_{bg} can vary for different types of bacteria.

The numerical model is implemented using MATLAB. At each time step the simulator plots the current concentrations of the species, saves the data in a separate file, and estimates the remaining time to completion.It includes a post-processor that uses the files created during a run and plots each one sequentially. It then creates a movie file in mpeg format for easy viewing of the results.

Situational adaptability. All rates, initial conditions, and other relevant parameters are easy to manipulate in order to create differing situations to model. Domain size, time interval, time step size, spatial step size, and other relevant parameters are also easy to manipulate to modify the accuracy of the model. The time step has an internal stability restriction, and it is cut if the specified step is too large.

Graphical user interface. The program contains a menu in the plot window that allows the user to select from a variety of display options. By default it makes a three dimensional mesh for each species and layer.

In the mesh mode, the user can select which layers to display, as well as the option of combining all layers of the same type to minimize the number of redundant graphs. They also have a range of scaling options to facilitate intelligibility of data.

It also has a cross-sectional view, in which the user has the option of choosing where the cross-section is taken as well as which axis to take it on. This mode also displays a layout of the section, showing the spatial arrangement of the compartments.

In all cases the user has the option of which species to display.

4.1 Case 1

In this case we begin with damaged wall to determine the effect of bacteria on the ability of the wall to close. We present two tests where we vary level of initial infection between the two trials. The initial condition in the first trial is shown in Figure 2. The initial condition in the second trial looks similar, except for the higher level of bacteria.

In the first trial we began with a small quantity of bacteria. The results of the simulation are shown in Figure 3. Although the the infection progresses into the

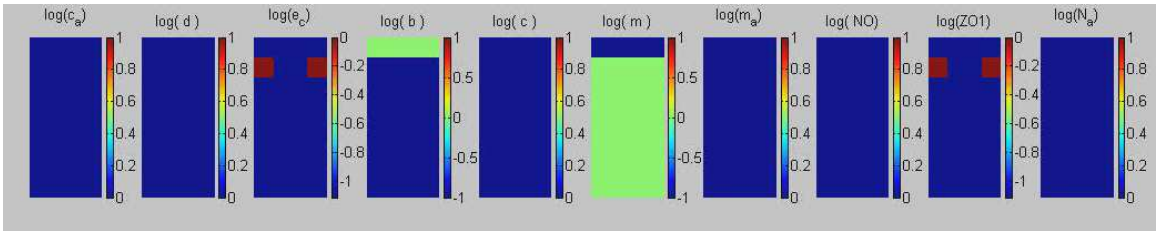

Figure 2: Initial condition for Case 1: uniform infection and damaged wall.

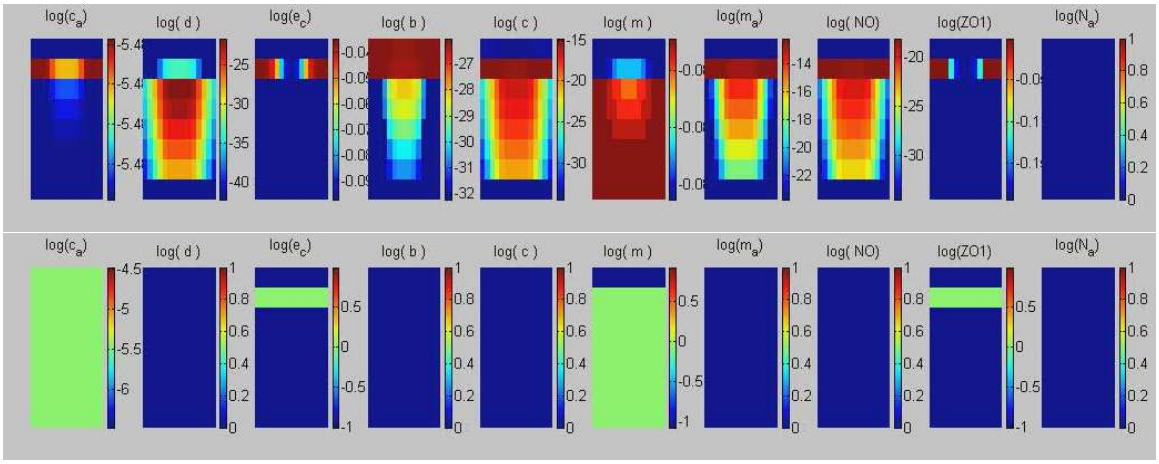

Figure 3: Simulation results for Case 1 with small initial infection. Top picture: state at early time; bottom picture: state at the end of the simulation

system as it can be seen in the top image, at the end the organ wall has healed completely and the bacteria is no longer present within the organ - the bottom image.

In the second trial we begin with a high level of infection. The top image in Figure 4 shows the progress of the infection. The wall has not been able to close around the infection due to the bacteria preventing the epithelial cells from migrating. The hole closes after the bacteria is killed, although residual inflammation processes continue for some time after that, as shown in the bottom image.

4.2 Case 2

In this case we begin with a healthy organ wall and only a point source of infection. We compare the assaults of bacteria with differing virulence by changing the reproduction rate of the bacteria. The initial condition for both tests is shown in Figure 5.

In the first trial we start with a relatively tame bacteria strain, and can see that the infection initially progresses into the system, see the top image in Figure 6. The infection is later controlled by the body and the bacteria has been cleared at the end, see the bottom image in Figure 6.

In the second trial we begin with a much more virulent bacteria. The top image

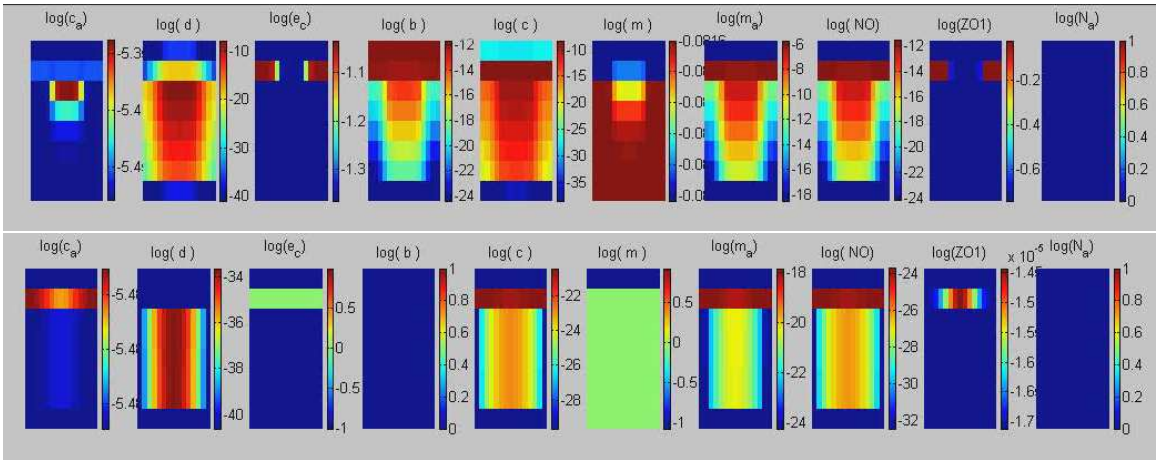

Figure 4: Simulation results for Case 1 with large initial infection. Top picture: state at early time; bottom picture: state at the end of the simulation

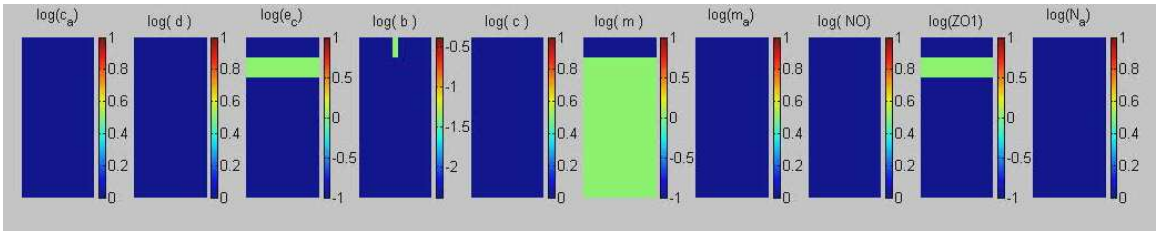

Figure 5: Initial condition for Case 2: point infection and healthy wall.

in Figure 7 shows that this bacteria has also penetrated the wall, but has created significantly more inflammation than the more tame version. The bottom image shows that the inflammation has gotten out of control.

5 Conclusions and future work

We have developed a mathematical and numerical model of inflammation that at least qualitatively simulates the body's response to infection. This model contains a large number of parameters that need to be verified experimentally before it can be expected to produce accurate results. These parameters include the rates of reactions, diffusion and advection rates, etc.

When we have a correct set of parameters it will provide us with insight into not only the processes of the immune system, but possibly with warning signs of failure.

These results can then help to predict when there is a problem and with these predictions treatments might be devised to stop the problem from getting out-of-control. In this way such maladies as NEC and sepsis might become avoidable, or possibly curable.

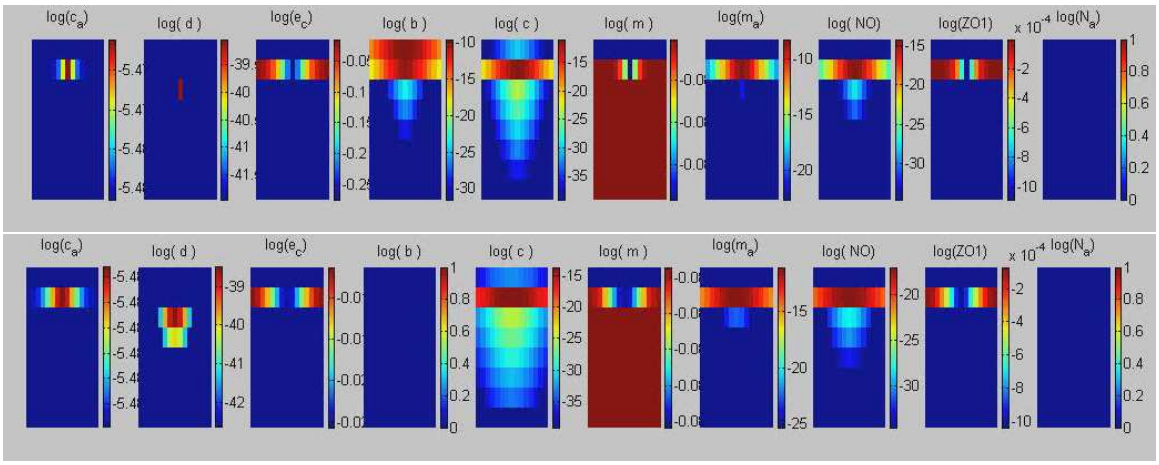

Figure 6: Simulation results for Case 2 with tame bacteria. Top picture: state at early time; bottom picture: state at the end of the simulation

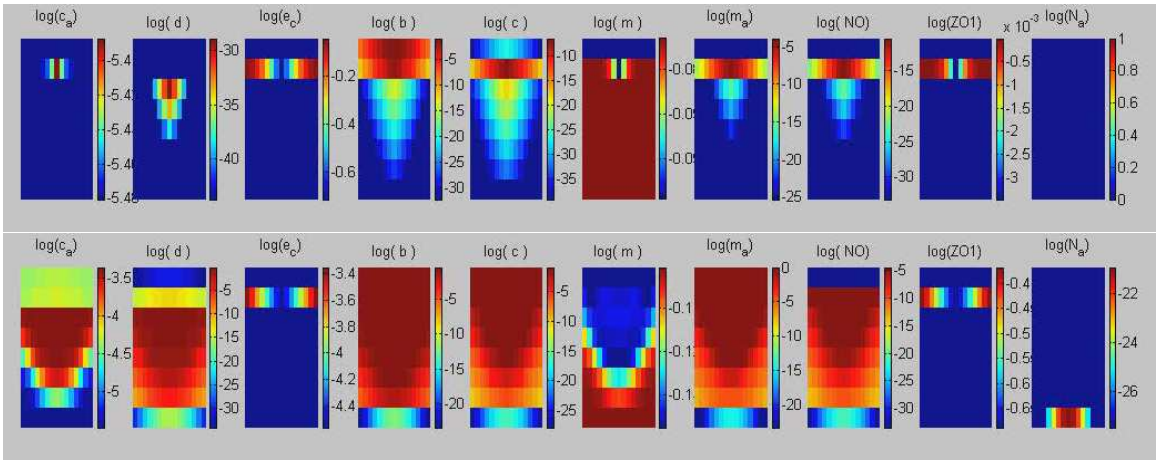

Figure 7: Simulation results for Case 2 with virulent bacteria. Top picture: state at early time; bottom picture: state at the end of the simulation

6 Acknowledgements

The authors would like to thank G. Clermont, J. Day, B. Ermentrout, D. Hackam, Q. Mi, A. Reynolds, B. Riviere, J, Rubin, D. Swigon, J. Upperman, Y. Vodovotz, and R. Zamora, members of the NEC-modeling group at University of Pittsburgh, for their valuable input in the development of the model.

References

[1] G. An. Agent-based computer simulations and SIRS: building a bridge between basic science and clinical trials. *Shock*, 16:266–273, 2001.

[2] G. Chavent and J. Jaffre. *Mathematical models and finite elements for reservoir simulation*. North-Holland, Amsterdam, 1986.

[3] G. Clermont, C. C. Chow, and G. M. Constantine. Mathematical and statistical modeling of acute inflammation. *Proc. Int. Fed. Classific. Soc.*, 2004.

[4] X. Han, M. Fink, and R. Delude. Proinflammatory cytokines cause NO-dependent and -independent changes in expression and localization of tight junction proteins in intestinal epithelial cells. *Shock*, 19(3):229–237, 2003.

[5] R. S. Hotchkiss and E. Karl. The pathophysiology and treatment of sepsis. *N. Engl. J. Med.*, 348(2):138–150, 2003.

[6] F. Qureshi, C. Leaphart, S. Cetin, J. Li, , A. Grishin, S. Watkins, H. Ford, and D. Hackam. Increased expression and function of integrins in enterocytes by endotoxin impairs epithelial restitution. Preprint.

[7] A. Reynolds, J. Rubin, G. Clermont, J. Day, and B. Ermentrout. Modeling the role of anti-inflammation in the acute immune response. *Journal of Critical Care*, 2005.

[8] A. Reynolds, J. Rubin, G. Clermont, J. Day, Y. Vodovotz, and B. Ermentrout. A reduced mathematical model of the acute inflammatory response. i. derivation of model and analysis of anti-inflammation. In review.

[9] Y. Vodovotz, C. Chow, J. Bartels, C. Lagoa, R. Kumar, J. Day, J. Rubin, B. Ermentrout, B. Riviere, I. Yotov, G. Constantine, T. Billiar, M. Fink, and G. Clermont. Mathematical simulations of sepsis and trauma. In *11th Congress of the European Shock Society*, pages 151–159. Medimond, 2005.

[10] Y. Vodovotz, G. Clermont, C. C. Chow, and G. An. Mathematical models of the accute inflammatory response. *Current Opinion in Critical Care*, 10:383–390, 2004.